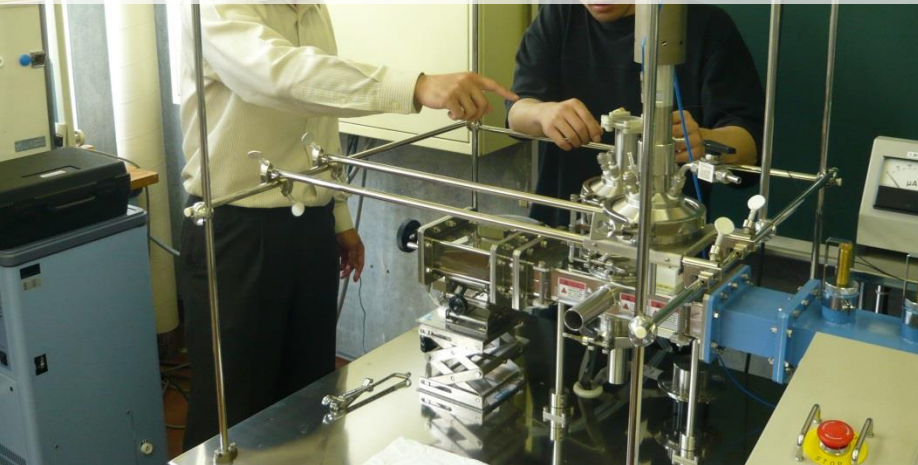


Uncertainty Analysis for S_{11} Calibration of a Coaxial Line with Three Reference Materials without Short Termination

Kouji Shibata

Department of Electric and Electronic Engineering,
Hachinohe Institute of Technology, Japan

Material heating system using waveguide components for effective synthesis of new chemical materials based on exposure of electromagnetic waves (Microwave chemistry)



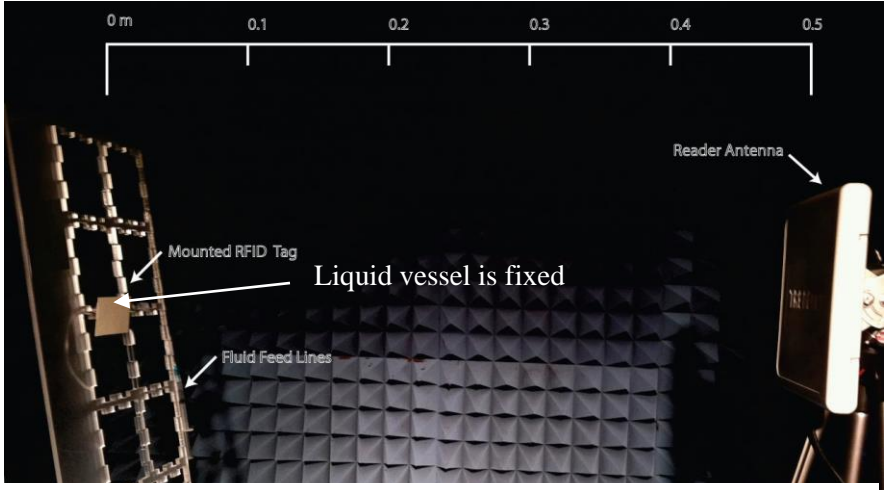
Microwave synthesis the aspirin and another medicines at short times effectively

Microwave roasted green tea

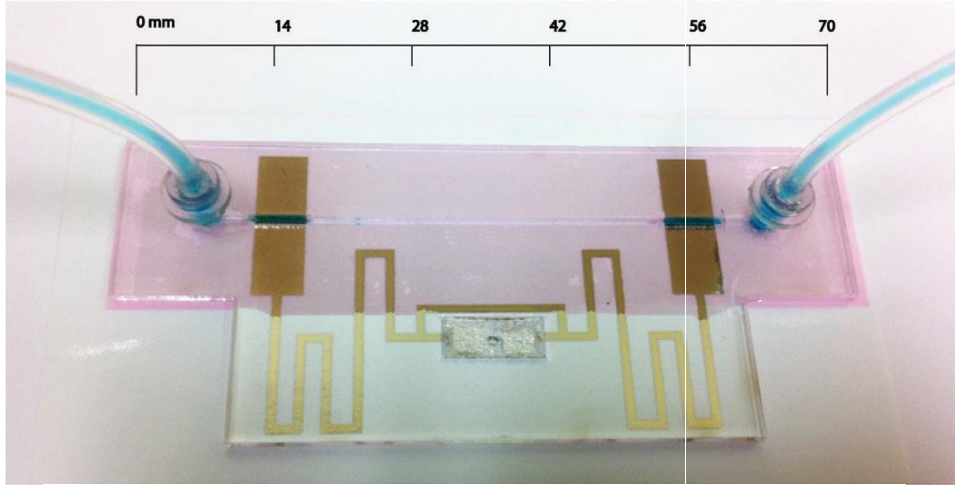
These studies have attached attention as boundary area research

Measurement of exact material constants for objects to be heated in the frequency band of EM wave exposure is very important for evaluation of characterization for the new materials by the effective synthesis

Evaluation of the RF-tag performance at UHF band using liquids as reference materials for humans in close proximity to IC tags



(a) Measurement in radio wave darkroom



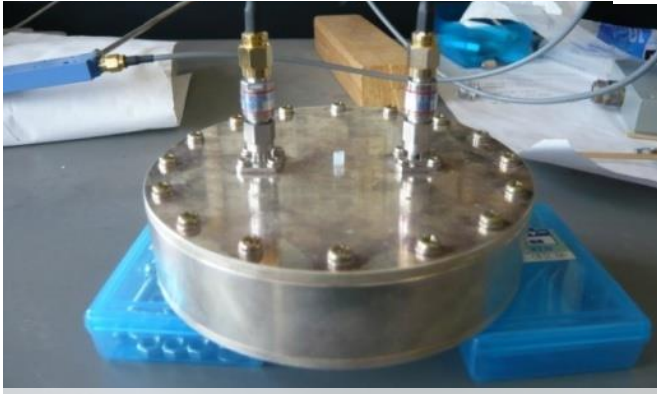
(b) Evaluation of RF tag using a liquid

Fabricated RFID-based microfluidic tag with printed antenna, laser-cut channel and printed bonding layer
Measurement setup for wireless measurements with immersing the RFID reader into a liquid

Cook, B.S., Cooper, J.R., Sangkil Kim and Tentzeris M.M. "A novel passive microfluidic RFID-based sensing platform" IEEE MTT-S International Microwave Symposium IMS2013 Digest, 2-7 June 2013, pp.1- 3.

Accurate measurement of the dielectric property for liquid material characterization is important for performance evaluation of radio systems

Dielectric measurement method in liquids



The transmission constant measuring method
A. M. Nicolson and G.F. Ross, 1970.

can be adopted for broadband measurement, Require consideration for the influence of liquid spillage

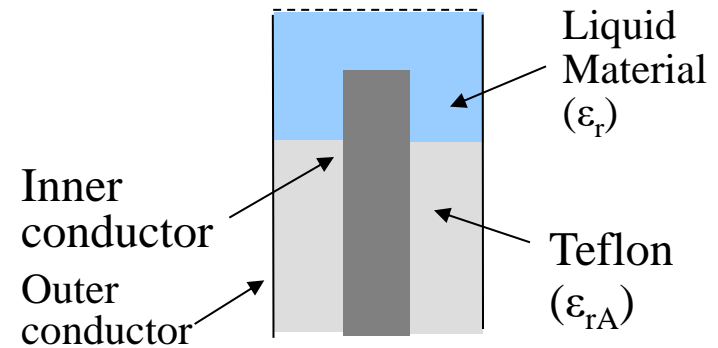
The cylindrical cavity resonator method

Does not support broadband measurement with a continuous frequency as this approach involves in response to the resonant frequency



The open coaxial probe method

Generally used for measurement of liquid.
A large amount of liquids is needed to avoid the influence of reflective waves from the vessel bottom



The coaxial line reflection method

O. Göttmann, U. Kaatze and P. Petong, 1996.

J.B. Javis, M.D. Janezic and C. A. Jones (NIST),

1998

Input Impedance greatly affects to the length of the coaxial line. There are many problems for standardization

Broadband measurement method of permittivity in liquids based on S_{11} using an open-ended cut-off circular waveguide (2010)

1. Measurement of the S_{11} at the reference plane when liquid is inserted into the open-ended measurement jig
2. The estimation of permittivity is performed by comparing the result of measured S_{11} value with calculated value of analytical model
3. The mode-matching method is applied for an analytical model

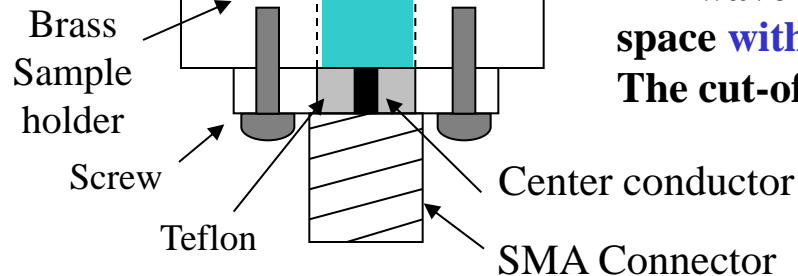


End of the waveguide is assumed to be in a perfect magnetic conductivity
This differs from termination condition of fabricated jig that can be used in practice
 Estimation of complex permittivity was performed as inverse problem using Newton-raphson method

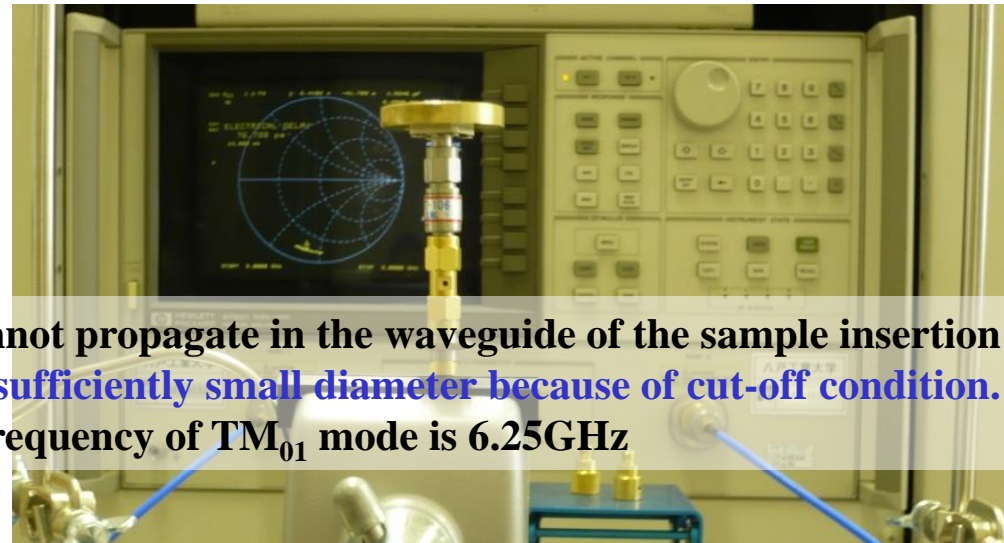
$$\dot{y}_m = j \cdot \frac{2k_0 a \cdot \dot{\epsilon}_r}{\sqrt{\epsilon_{rA}} \cdot \ln\left(\frac{a}{b}\right)} \left(y_0 - \sum_{q=1}^{\infty} y_q \cdot x_q \right)$$

EM is confined in the waveguide

Material filling space



EM wave cannot propagate in the waveguide of the sample insertion space with a sufficiently small diameter because of cut-off condition. The cut-off frequency of TM_{01} mode is 6.25GHz



Dimensions of the jig are $2a=4.1\text{mm}$, $2b=1.3\text{mm}$, $d=5.0\text{mm}$ and $\epsilon_{rA}=2.05$

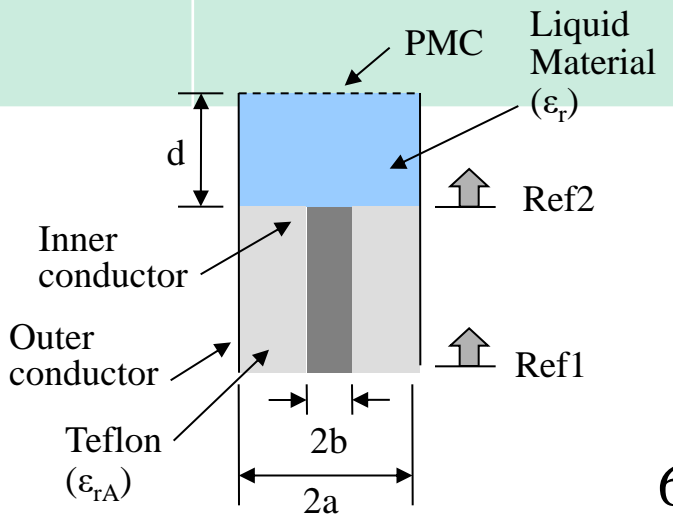
Classification of liquid permittivity estimation methods via the open-end cut-off circular waveguide reflection method

Method	Advantage	Week point	Remarks
Inverse problem via the EM analysis (mode-matching method) for analytical model [1]	Exact estimation is possible by performing exact S_{11} calculations for the analytical model	Certain amount of computer resources are required	
Estimation formula compared with short, open and one reference material [2]	Simple dielectric measurement using estimation formula	Error caused by approximation using equivalent circuit	Applied to conventional coaxial probe such as KEYSIGHT Technologies
Estimation formula compared with three reference materials [3]	Easy estimation with equation Comparison with short termination is not required Movement of observation plane from SOL calibration plane (Ref. 1) to sample front (Ref. 2) is not required	Error caused by approximation using equivalent circuit	

[1] K. Shibata, "Measurement of Complex Permittivity for Liquid Materials Using the Open-ended Cut-off Waveguide Reflection Method," IEICE Trans. Electron., Vol. E93-C, No. 11, pp. 1621 – 1629, 2010-11.

[2] K. Shibata and M. Kobayashi, "Simplification of Liquid Dielectric Property Evaluation Based on Comparison with Reference Materials and Electromagnetic Analysis Using the Cut-off Waveguide Reflection Method," IEICE Trans. Electron., Vol. E100-C, No. 10, pp. 908-917, 2017-10.

[3] K. Shibata, "Dielectric Measurement in Liquids Using an Estimation Equation without Short Termination via the Cut-Off Circular Waveguide Reflection Method," IEICE Trans. Electron., vol.E101-C, no.8, pp. 627 – 636, 2018-8.



S_{11} Calculation via the mode-matching technique

For fast computation of the S_{11} of the analytical model at the reference plane

Formulation was performed using the Galerkin method based on the orthogonality of the Bessel function to simultaneous equations.

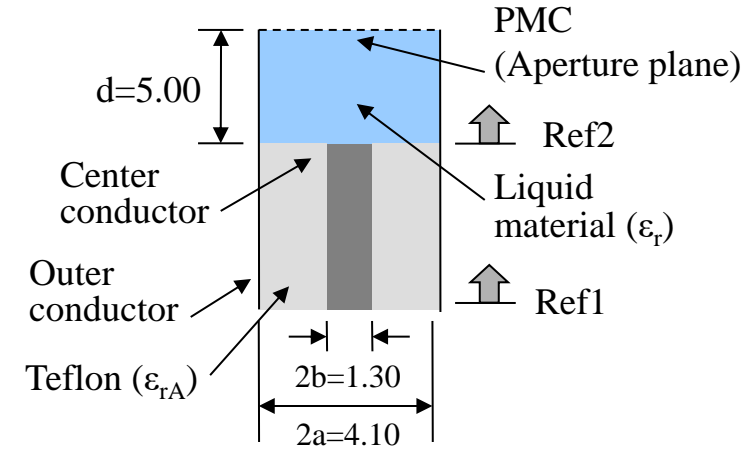
These equations were obtained by applying the continuity condition to the tangential components of EM components (In this case, TM mode for each region)

$$\dot{y}_m = j \cdot \frac{2k_0 a \cdot \dot{\epsilon}_r}{\sqrt{\epsilon_{rA}} \cdot \ln\left(\frac{a}{b}\right)} \left(y_0 - \sum_{q=1}^{\infty} y_q \cdot x_q \right)$$

$$x_q = A_{qn}^{-1} \cdot y_q \quad y_0 = \sum_{i=1}^{\infty} \frac{\tanh\left[(\lambda_i^2 a^2 - k^2 a^2)^{1/2} d / a\right] \cdot J_0^2(\lambda_i \cdot b)}{(\lambda_i^2 a^2 - k^2 a^2)^{1/2} \lambda_i^2 a^2} \cdot \frac{J_0^2(\lambda_i \cdot b)}{J_1^2(\lambda_i \cdot a)}$$

$$A_{qn} = \sum_{i=1}^{\infty} \frac{\lambda_i^2 a^2 \cdot \tanh\left[(\lambda_i^2 a^2 - k^2 a^2)^{1/2} d / a\right]}{(\lambda_i^2 a^2 - k^2 a^2)^{1/2} (\lambda_i^2 a^2 - \xi_q^2 a^2) \cdot (\lambda_i^2 a^2 - \xi_n^2 a^2)} \cdot \frac{J_0^2(\lambda_i \cdot b)}{J_1^2(\lambda_i \cdot a)} + \frac{1}{\dot{\epsilon}_r} \cdot \frac{\delta_{qn}}{4(\xi_n^2 a^2 - k_0^2 a^2 \cdot \epsilon_{rA})^{1/2}} \cdot \left[\frac{a^2}{b^2} \cdot \frac{Z_1^2(\xi_n \cdot a)}{Z_1^2(\xi_n \cdot b)} - 1 \right]$$

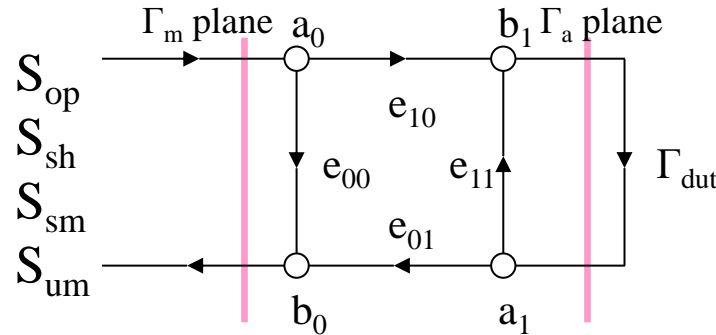
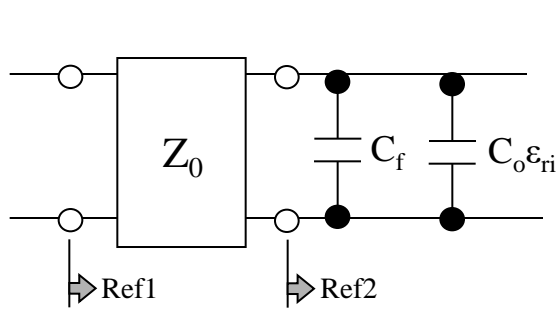
$$y_q = - \sum_{i=1}^{\infty} \frac{\tanh\left[(\lambda_i^2 a^2 - k^2 a^2)^{1/2} d / a\right] \cdot J_0^2(\lambda_i \cdot b)}{(\lambda_i^2 a^2 - k^2 a^2)^{1/2} (\lambda_i^2 a^2 - \xi_q^2 a^2)} \cdot \frac{J_0^2(\lambda_i \cdot b)}{J_1^2(\lambda_i \cdot a)}, \quad J_0(\xi_q a) \cdot N_0(\xi_q b) - J_0(\xi_q b) \cdot N_0(\xi_q a) = 0$$



The calculation time is about one second for each frequency

Fast estimation of the complex permittivity can be performed

Simplification of dielectric measurement procedure using an estimation equation compared with short, open and one kind reference material



Applied to
conventional
coaxial probe
such as
KEYSIGHT
Technologies

Derived from the equivalent circuit from three termination conditions

$$\dot{\epsilon}_{rm} = \frac{\dot{\epsilon}_{ra} (\dot{S}_{11m} - \dot{S}_{11o}) (\dot{S}_{11s} - \dot{S}_{11a}) + (\dot{S}_{11m} - \dot{S}_{11a}) (\dot{S}_{11o} - \dot{S}_{11s})}{(\dot{S}_{11m} - \dot{S}_{11s}) (\dot{S}_{11o} - \dot{S}_{11a})}$$

S_{11s} : Measured S_{11} under the condition that tip of the jig is **short**

S_{11o} : Measured S_{11} under the condition that tip of the jig is **open**

ϵ_{ra} : Complex **permittivity** of reference material for comparison

S_{11a} : Measured S_{11} when **reference** material is inserted for comparison

S_{11m} : Measured S_{11} when **unknown material is** inserted

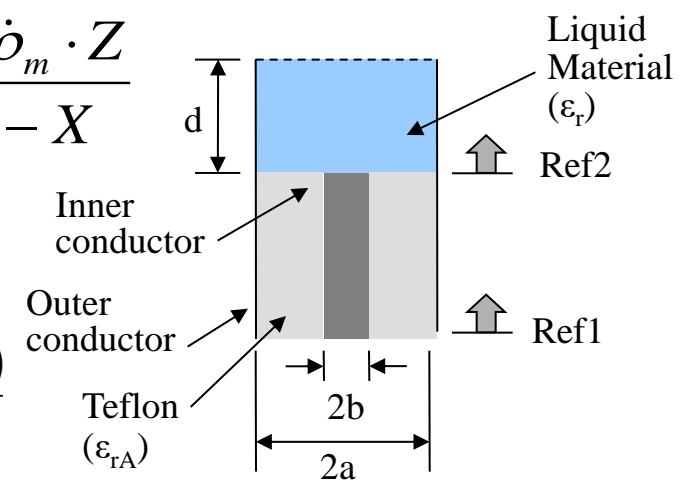
ϵ_{rm} : **Estimated** result of **complex permittivity** for unknown material

Complex permittivity estimation formula for unknown material comparing with three reference materials and with no short termination

$$\dot{\epsilon}_{rm} = \frac{Y - \dot{\rho}_m \cdot Z}{\dot{\rho}_m - X}$$

$$X = \frac{\dot{\rho}_1 \cdot \dot{\rho}_3 \cdot (\dot{\rho}_2 - \dot{\rho}_1) \cdot (\dot{\epsilon}_{r1} - \dot{\epsilon}_{r3}) + \dot{\rho}_1 \cdot \dot{\rho}_2 \cdot (\dot{\rho}_3 - \dot{\rho}_1) \cdot (\dot{\epsilon}_{r2} - \dot{\epsilon}_{r1})}{(\dot{\rho}_2 - \dot{\rho}_1) \cdot (\dot{\rho}_3 \cdot \dot{\epsilon}_{r1} - \dot{\rho}_1 \cdot \dot{\epsilon}_{r3}) - (\dot{\rho}_3 - \dot{\rho}_1) \cdot (\dot{\rho}_2 \cdot \dot{\epsilon}_{r1} - \dot{\rho}_1 \cdot \dot{\epsilon}_{r2})}$$

$$Y = \frac{(\dot{\rho}_1 \cdot \dot{\epsilon}_{r2} - \dot{\rho}_2 \cdot \dot{\epsilon}_{r1}) \cdot X + \dot{\rho}_1 \cdot \dot{\rho}_2 \cdot (\dot{\epsilon}_{r1} - \dot{\epsilon}_{r2})}{\dot{\rho}_2 - \dot{\rho}_1}, \quad Z = \frac{Y + \dot{\epsilon}_{r1} \cdot (X - \dot{\rho}_1)}{\dot{\rho}_1}$$



ϵ_{rm} is determined from ϵ_{r1} , ϵ_{r2} , ϵ_{r3} , ρ_1 , ρ_2 , ρ_3 and ρ_m (reflection constant of unknown material)

ϵ_{ra1} : Complex permittivity of **first** reference material for comparison

S_{11a1} : Measured value of S_{11} when **first** reference material is inserted

ϵ_{ra2} : Complex permittivity of **second** reference material for comparison

S_{11a2} : Measured value of S_{11} when **first** reference material is inserted

S_{11o} : Measured value of S_{11} when liquid material is **not inserted (open)**

S_{11m} : Measured value of S_{11} when **unknown material** is inserted

ϵ_{rm} : Estimated value of complex permittivity for **unknown material**

Advantage: there is no need to move the reference plane after SOL calibration with the calibration kit because the short is not used as the reference

Problems and improvements over previous methods

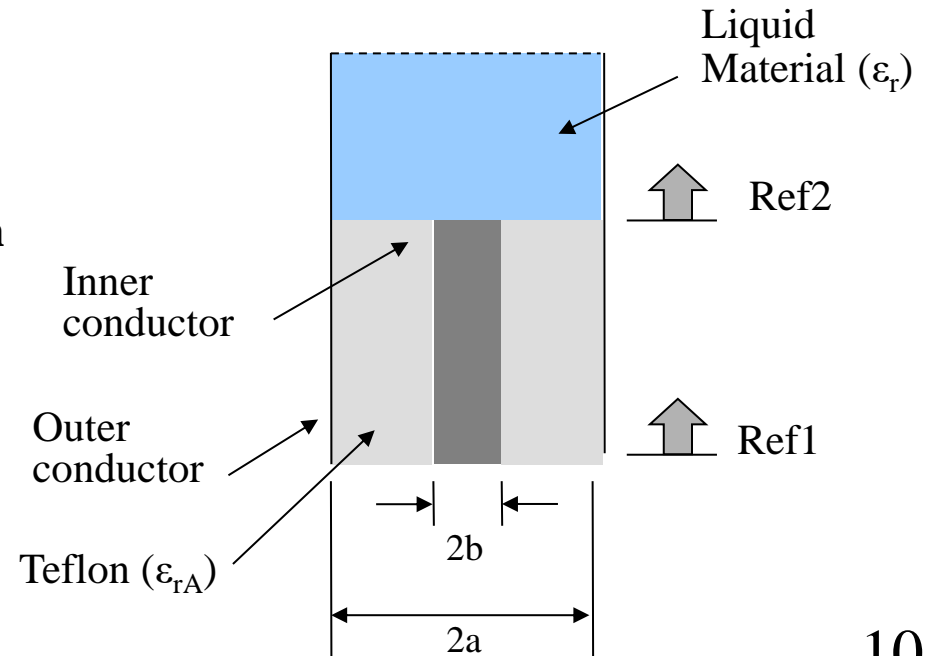
1. The dynamic range was improved by setting the appropriate IF Bandwidth and the averaging factor when measuring S_{11} using a vector network analyzer
2. The observation surface (Ref surface) of S_{11} was determined by moving from the SOL calibration plane to the sample front using the electrical delay function of VNA

In that case, The amount of movement of the observation plane was determined visually using a Smith chart. An error occurred in the measured value of S_{11} and the estimated value of the permittivity due to the variation in the amount of phase shift, especially at high frequencies

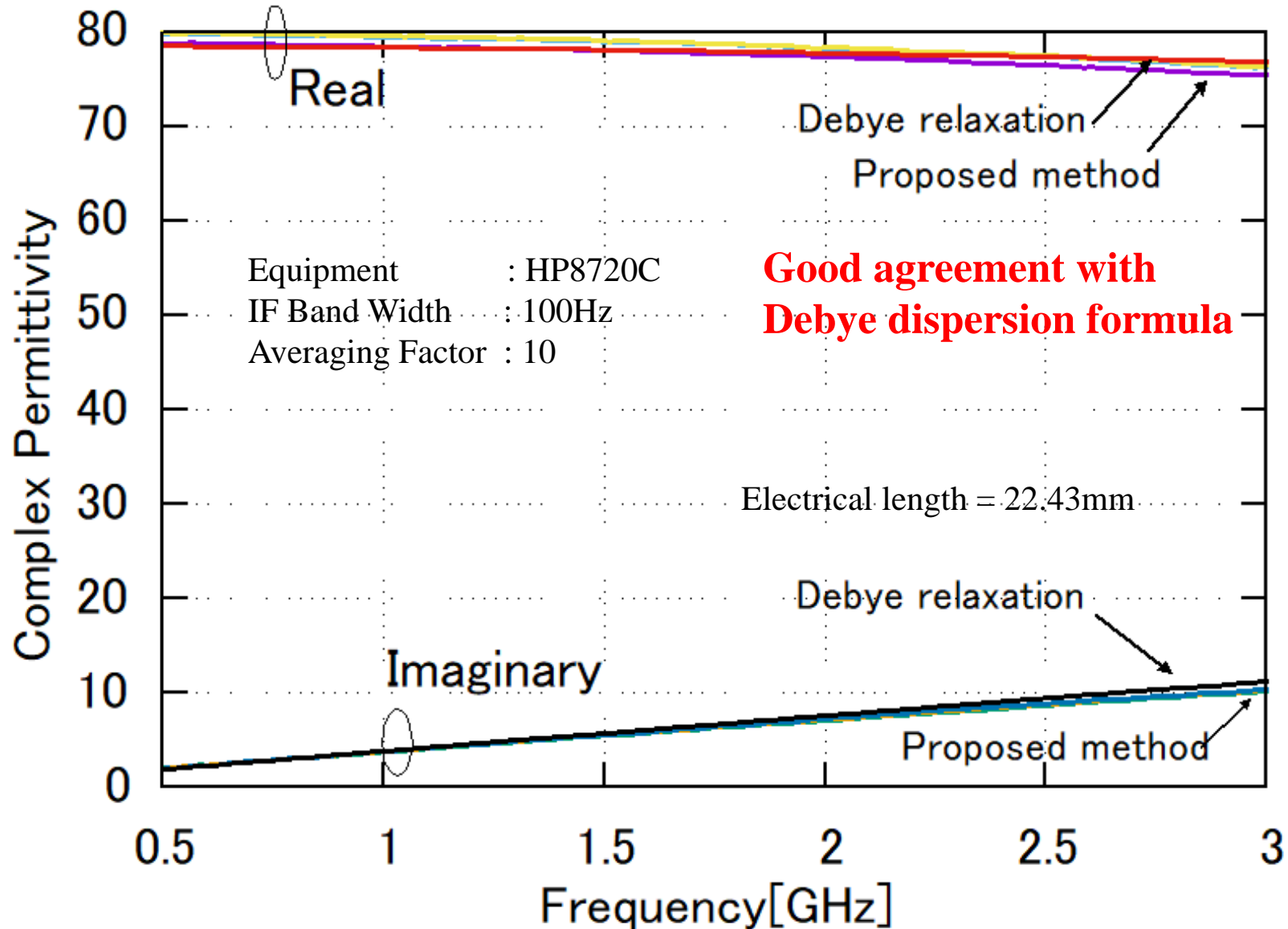
Accordingly

The procedure for determining the reference plane by comparing the calculated S_{11} value via the EM analysis under the open condition with the measured value was applied

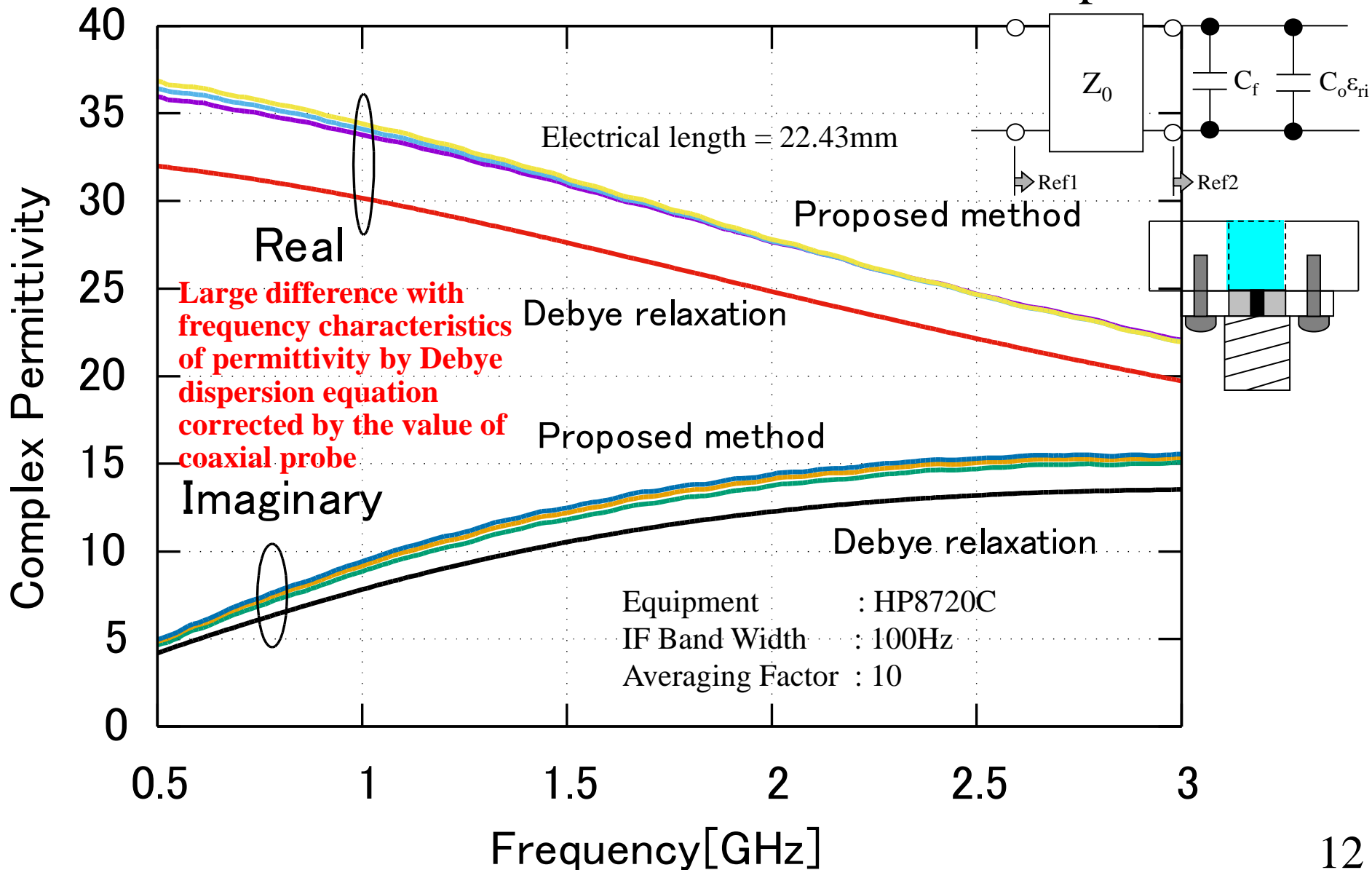
As a result, measurement accuracy of dielectric constant at high frequencies was improved



Complex permittivity of **pure water** using the measurement jig with SMA connector after moving the electrical length of S_{11} from the SOL calibration surface to the sample front



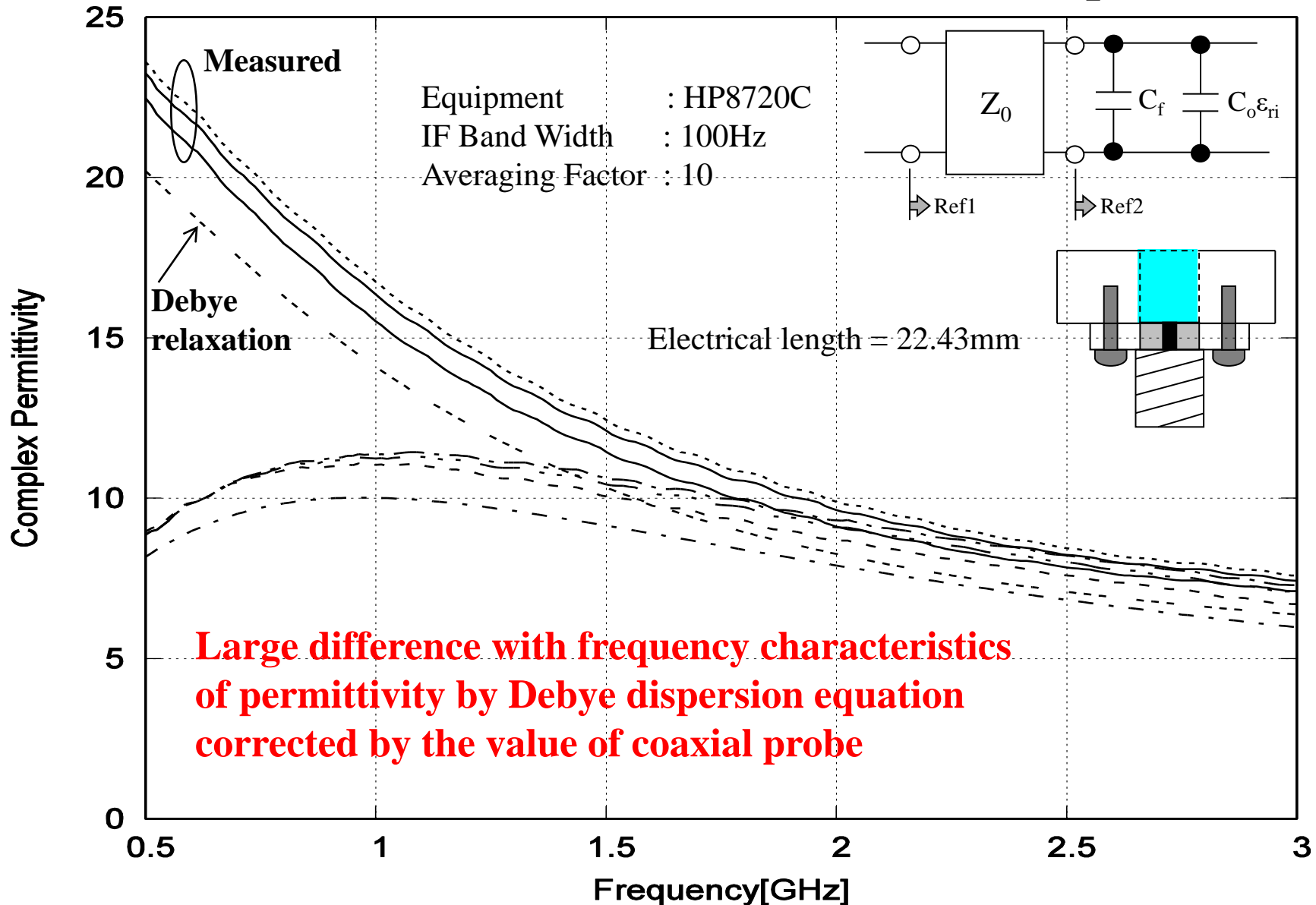
Complex permittivity of **methanol** using the measurement jig with SMA connector after moving the electrical length of S_{11} from the SOL calibration surface to the sample front



The difference of 9% or more also seen for both the real and imaginary is attributed to two factors relating to the sample insertion part of the jig being in an open state

1. Incorporation of airborne moisture into methanol
2. Reduction of liquid temperature caused by liquid evaporation after insertion into the jig.

Complex permittivity of ethanol using the measurement jig with SMA connector after moving the electrical length of S_{11} from the SOL calibration surface to the sample front



Comparison of each dielectric measurement method

	Cavity resonator	Nicolson and Ross	Open-ended coaxial line	Coaxial probe	Open-ended cutoff-waveguide
Broad band	×	○	△	△	△
Ease of measurement	△	△	○	○	○
Small quantity	○	○	○	×	○
Accuracy	○ (Exact solution)	○	○	△ (Quasi electrostatic field approximation)	○ (Exact solution)
Absolute measurement	○	○	○	△	○

At low frequency, measuring precision is deteriorated by the fluctuations of S_{11}

Relative measurement based on the pure water (by Agilent)

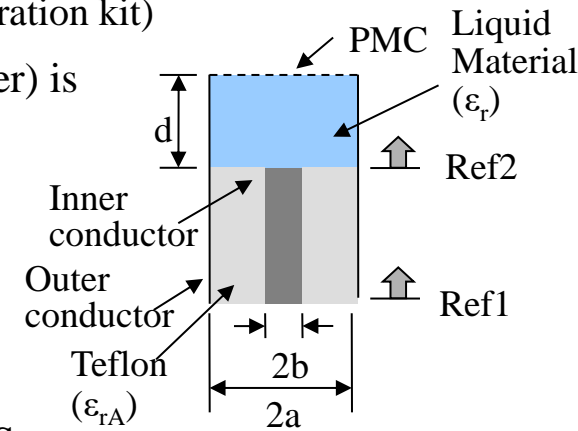
Present method can respond to the needs for a small amount of liquids by using a cheap measurement jig in a broad frequency range

Great variability of measurement values can be seen at low frequency

Factors adversely affecting measurement uncertainty with cut-off circular waveguide reflection

Measurement condition (S_{11} is calibrated by a commercially available SOL calibration kit)

1. S_{11} at the tip of a coaxial line connected to a VNA (vector network analyzer) is calibrated using a calibration kit with SOL conditions before jig mounting
2. The jig is attached to the coaxial tip. Next, S_{11} on the SOL calibration surface (Ref. 1) is measured with each unknown material
3. The electrical length as measured above is moved to the front surface of the sample (Ref. 2)
4. The permittivity is estimated as an inverse problem so that the calculated S_{11} value for the analytical model composed of a jig corresponds to the measured value



No.	Item	Function
1	Input impedance difference between measured and true values (real part)	$u(x_1)$
2	Input impedance difference between measured and true values (imaginary part)	$u(x_2)$
3	Difference from the true value of the outer conductor diameter $2a$	$u(x_3)$
4	Difference from the true value of the center conductor diameter $2b$	$u(x_4)$
5	Observation surface difference from the sample front	$u(x_5)$
6	Changes in S_{11} (complex permittivity) due to changes in liquid temperature	$u(x_6)$
7	Error from convergence of the EM analysis value for S_{11} (from the number of expansion terms q)	$u(x_7)$
8	Error from convergence of the EM analysis value for S_{11} (from the sample insertion part length d [mm])	$u(x_8)$
9	Difference from the theoretical value with a short calibrator	$u(x_9)$
10	Difference from the theoretical value with an open calibrator	$u(x_{10})$
11	Difference from the theoretical value with a matched-load calibrator	$u(x_{11})$

Calculation procedure of uncertainty in dielectric measurement

Based on the uncertainties of the items in the table, the combined standard measurement uncertainty for the real part of complex permittivity was calculated using Eq. (1) with the square root of the sum of the squares of each term (cumulative error)

$$u_c(\varepsilon_r') = \sqrt{\sum_{i=1}^n u_i^2(\varepsilon_r')} \quad (1)$$

Here, $u_i(\varepsilon_r')$ is the measurement error of the real part of complex permittivity for each term. $u_i(\varepsilon_r')$ is then calculated using Eq. (2).

$$u_i(\varepsilon_r') \equiv \left| \frac{\partial \varepsilon_r'}{\partial x_i} \right| \cdot u(x_i) \quad (2)$$

The combined standard measurement uncertainty for the imaginary part of the permittivity was also calculated using Eq. (3) as the square root of the sum of the squares of each term (i.e., the cumulative error)

$$u_c(\varepsilon_r'') = \sqrt{\sum_{i=1}^n u_i^2(\varepsilon_r'')} \quad (3)$$

$u_i(\varepsilon_r'')$ is the measurement error for the imaginary part of permittivity for each term. $u_i(\varepsilon_r'')$ is then calculated using Eq. (4)

$$u_i(\varepsilon_r'') \equiv \left| \frac{\partial \varepsilon_r''}{\partial x_i} \right| \cdot u(x_i) \quad (4)$$

$\partial \varepsilon_r' / \partial x_i$ in Eq. (2) and $\partial \varepsilon_r'' / \partial x_i$ in Eq. (4) are referred to as sensitivity coefficients. The small changes in relative permittivity associated with slight changes in individual items are then calculated by combining numerical calculation and numerical differentiation

$u(x_i)$ in Eqs. (2) and (4) is the measurement error of permittivity for each item. For example, the measurement error when the item deviates from the true value is expressed by Eq. (5) for the real part (relative permittivity) of the complex permittivity in Eq. (2).

$$u(x_i) = \varepsilon'_{r_var_i} - \varepsilon'_{r_ideal_i} \quad (5)$$

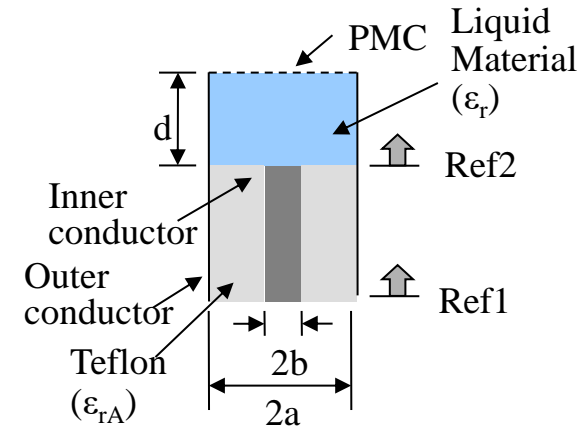
The differentiation procedure is outlined below

1. A program for estimating complex permittivity based on cut-off circular waveguide reflection as an inverse problem via the mode-matching method is created
2. The small change observed in complex permittivity when the real part of input impedance changes slightly with respect to the complex permittivity of pure water is calculated using the above program
3. The partial differential $\partial \varepsilon_r' / \partial x$ is calculated as the ratio (quotient) of $\partial \varepsilon_r'$ and ∂x
4. The absolute of $|\partial \varepsilon_r' / \partial x_i|$ for the $\partial \varepsilon_r' / \partial x$ value determined in 3 is calculated

Conditions for analysis of measurement uncertainty of complex permittivity

Theoretical values for the dielectric constant of the reference material (25°C) and input impedance at the front of the sample (Ref. 2)

Condition	Frequency [GHz]		
	0.50	1.5	3.0
Complex permittivity of pure water	78.504	78.108	76.803
	-j 1.912	-j 5.705	-j 11.206
Theoretical value from mode-matching with pure water in the jig Z_{1_ideal}	3.468596	3.469369	3.485887
	-j 142.7852	-j 46.7846	-j 21.9431



Dimension of jig and various electric constant $2a = 4.10\text{mm}$, $2b = 1.30\text{mm}$, $d = 5.00\text{mm}$, $\epsilon_{rA} = 2.05$

$u(x_1)$ and $x_1(x_1)$ due to the difference between true value and measured value of the input impedance (0.5GHz, permittivity of water: $78.504 - j 1.912$)

$$u_1(\epsilon_r') \equiv \left| \frac{\partial \epsilon_r'}{\partial x_1} \right| \cdot u(x_1), \quad u(x_1) = \epsilon'_{r_var_1} - \epsilon'_{r_ideal_1}, \quad \partial x_1 = \frac{R_{val} - R_{ini}}{R_{ini}} = \Delta x, \quad \partial \epsilon_r' = \frac{\epsilon_r'(x_1) - \epsilon_r'}{\epsilon_r'}$$

Condition	Frequency [GHz]		
	0.50	1.5	3.0
Deviation of the real part of input impedance from the true value	± 0.50	± 0.50	± 0.50
Input impedance when the real part deviates from the true value	3.9686 -j 142.785	3.9694 -j 46.7846	3.9859 -j 21.9431
Estimated complex permittivity with the above input impedance	78.489 -j 2.187	77.981 -j 6.517	76.318 -j 12.734
Real part of $u(x_1)$	$1.431 \cdot 10^{-2}$	0.1272	0.4844
Imaginary part of $u(x_1)$	0.2752	0.8116	1.528

Small rate of change Δx	0.02	0.03	0.04
Small change in the real part of input impedance ΔR	$6.9372 \cdot 10^{-2}$	0.1041	0.1387
Estimated complex permittivity at the above input impedance	78.502 -j 1.950	78.501 -j 1.969	78.500 -j 1.988
Partial differential for complex permittivity with the real part $ \partial \epsilon_r' / \partial x_1 $	$5.929 \cdot 10^{-4}$	$6.058 \cdot 10^{-4}$	$6.099 \cdot 10^{-4}$
Partial differential for complex permittivity with the imaginary part $ \partial \epsilon_r'' / \partial x_1 $	$2.434 \cdot 10^{-2}$	$2.434 \cdot 10^{-2}$	$2.434 \cdot 10^{-2}$
$u_1(x_1)$ (real part)	$8.485 \cdot 10^{-6}$	$8.671 \cdot 10^{-6}$	$8.729 \cdot 10^{-6}$
$u_1(x_1)$ (imaginary part)	$6.698 \cdot 10^{-3}$	$6.698 \cdot 10^{-3}$	$6.698 \cdot 10^{-3}$

The variation of the real part of the input impedance does not significantly affect the measured value of the real part of the complex permittivity

Budget sheet and calculation of combined standard uncertainty in complex permittivity measurement for pure water using the cut-off circular waveguide reflection method (25.0°C, $\Delta x=0.03$)

Real

Imaginary

Condition	Frequency [GHz]			Condition	Frequency [GHz]		
	0.50	1.5	3.0		0.50	1.5	3.0
$ \partial \epsilon_r' / \partial x_1 \cdot U(x_1)$	$1.851 \cdot 10^{-5}$	$1.468 \cdot 10^{-3}$	$2.156 \cdot 10^{-2}$	$ \partial \epsilon_r'' / \partial x_1 \cdot U(x_1)$	$1.339 \cdot 10^{-2}$	0.1176	0.4319
$ \partial \epsilon_r' / \partial x_2 \cdot U(x_2)$	-0.6482	-1.906	-3.404	$ \partial \epsilon_r'' / \partial x_2 \cdot U(x_2)$	$-7.397 \cdot 10^{-4}$	$-1.982 \cdot 10^{-2}$	-0.1433
$ \partial \epsilon_r' / \partial x_3 \cdot U(x_3)$	$-7.738 \cdot 10^{-2}$	$-5.698 \cdot 10^{-2}$	$-8.960 \cdot 10^{-3}$	$ \partial \epsilon_r'' / \partial x_3 \cdot U(x_3)$	$1.368 \cdot 10^{-7}$	$4.087 \cdot 10^{-5}$	$-5.142 \cdot 10^{-4}$
$ \partial \epsilon_r' / \partial x_4 \cdot U(x_4)$	0.8802	0.8613	0.7937	$ \partial \epsilon_r'' / \partial x_4 \cdot U(x_4)$	$-5.825 \cdot 10^{-7}$	$-4.424 \cdot 10^{-5}$	$-8.052 \cdot 10^{-4}$
$ \partial \epsilon_r' / \partial x_5 \cdot U(x_5)$	0.1317	0.2349	0.5179	$ \partial \epsilon_r'' / \partial x_5 \cdot U(x_5)$	$-1.313 \cdot 10^{-5}$	$4.365 \cdot 10^{-5}$	$1.080 \cdot 10^{-2}$
$ \partial \epsilon_r' / \partial x_6 \cdot U(x_6)$	$4.060 \cdot 10^{-2}$	$3.677 \cdot 10^{-2}$	$2.527 \cdot 10^{-2}$	$ \partial \epsilon_r'' / \partial x_6 \cdot U(x_6)$	$1.068 \cdot 10^{-3}$	$9.401 \cdot 10^{-3}$	$3.515 \cdot 10^{-2}$
$ \partial \epsilon_r' / \partial x_7 \cdot U(x_7)$	$2.931 \cdot 10^{-4}$	$2.882 \cdot 10^{-4}$	$2.687 \cdot 10^{-4}$	$ \partial \epsilon_r'' / \partial x_7 \cdot U(x_7)$	$-7.560 \cdot 10^{-9}$	$-5.709 \cdot 10^{-8}$	$-4.274 \cdot 10^{-8}$
$ \partial \epsilon_r' / \partial x_8 \cdot U(x_8)$	$-1.310 \cdot 10^{-5}$	$-1.825 \cdot 10^{-5}$	$-7.092 \cdot 10^{-5}$	$ \partial \epsilon_r'' / \partial x_8 \cdot U(x_8)$	$7.659 \cdot 10^{-11}$	$3.274 \cdot 10^{-8}$	$3.011 \cdot 10^{-6}$
$ \partial \epsilon_r' / \partial x_9 \cdot U(x_9)$	$3.826 \cdot 10^{-2}$	$2.919 \cdot 10^{-2}$	$7.504 \cdot 10^{-3}$	$ \partial \epsilon_r'' / \partial x_9 \cdot U(x_9)$	$5.203 \cdot 10^{-3}$	$4.462 \cdot 10^{-2}$	0.1707
$ \partial \epsilon_r' / \partial x_{10} \cdot U(x_{10})$	-0.2030	$9.855 \cdot 10^{-2}$	$5.882 \cdot 10^{-2}$	$ \partial \epsilon_r'' / \partial x_{10} \cdot U(x_{10})$	-0.3083	-6.921 $\cdot 10^{-3}$	-1.478 $\cdot 10^{-2}$
$ \partial \epsilon_r' / \partial x_{11} \cdot U(x_{11})$	0.6265	0.5867	0.4987	$ \partial \epsilon_r'' / \partial x_{11} \cdot U(x_{11})$	$2.887 \cdot 10^{-4}$	$1.082 \cdot 10^{-3}$	$2.686 \cdot 10^{-4}$
Combined standard uncertainty (Real)	1.288	2.188	3.569	Combined standard uncertainty (imaginary)	0.1096	0.2962	1.050
	78.504 ± 1.288	78.108 ± 2.188	76.803 ± 3.569		1.912 ± 0.1096	5.705 ± 0.2962	11.206 ± 1.050

These phenomenon's are also affected from the uncertainty due to deterioration of S_{11}

The measurement uncertainty of **the real part of the complex permittivity** is greatly affected by the difference from the true value of the imaginary part of the input impedance ($u(x_2)$), the difference of the center conductor diameter $2b$ ($u(x_4)$) and the load calibrator ($u(x_{11})$)

The uncertainty of **the imaginary part** is greatly affected by the difference between the real part of the input impedance ($u(x_1)$) and the theoretical value of the open calibrator ($u(x_{10})$)

Uncertainties in both real and imaginary parts worsened as frequency increased

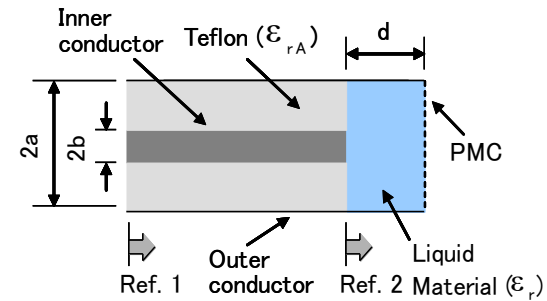
From the above study, the factor of worsening uncertainty when measuring the permittivity of liquids by the cut-off circular waveguide reflection method was clarified quantitatively. 20

Problems of conventional dielectric measurement methods

On the previous dielectric measurement method, the tip of the coaxial cable is first calibrated with a SOL calibration jig before mounting the jig

Next, the jig is mounted and the reference plane (electrical length) is moved to the front of the sample

Finally, the complex permittivity can be estimated by comparing the measured values of S_{11} of various liquids with those of S_{11} by the EM analysis



At that time, **S_{11} is not calibrated at the tip after jig is attached**

Accordingly, measurement error of S_{11} is occurred due to jig size variation

A measurement error of S_{11} is occurred due to the difference in the set value of the electrical length when moving the observation plane from the SOL calibration plane to the sample front

→ **Factors that deteriorate measurement accuracy (uncertainty) of dielectric constant**

S_{11} of the measurement jig should be calibrated in front of the sample

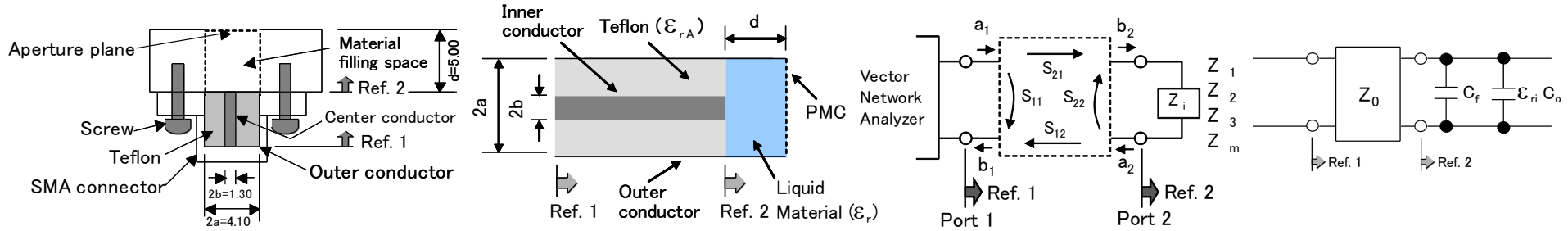
However, the realization of the short termination is challenging

This study

Evaluation of the uncertainty of measured values when S_{11} is calibrated at jig tip with three reference materials without using short termination

In near future, study on the effect of the above uncertainty of S_{11} on the uncertainty of the estimated result of the complex permittivity of various liquids by the cut-off circular waveguide reflection method is required

Calibration Method of S_{11} for Coaxial Line with Three Reference Material and no short condition, and Analytical Model of Measurement Uncertainty



The calculation formula of measured value of the reflection coefficient Γ_{corr} for Ref. 2 (Port 2) obtained from the measurement value ρ_{meas} of the reflection coefficient for Ref. 1 (Port 1) when inserting an unknown material is as shown on the right side.

$$\dot{\Gamma}_{corr} = \frac{a_2}{b_2} = \frac{\dot{\rho}_{meas} - \dot{E}_{DF}}{\dot{E}_{RF} + \dot{E}_{SF} \cdot (\dot{\rho}_{meas} - \dot{E}_{DF})}$$

Here, an error term for determination of the calibration condition is as follows

$$E_{SF} = \frac{\dot{\rho}_2 - \dot{\rho}_3 + \gamma \cdot (\dot{\Gamma}_3 - \dot{\Gamma}_2)}{\dot{\Gamma}_2 \cdot \dot{\rho}_2 - \dot{\Gamma}_3 \cdot \dot{\rho}_3}, E_{DF} = \dot{\rho}_1 - \dot{\Gamma}_1 \cdot (E_{SF} \cdot \dot{\rho}_1 + \gamma), E_{RF} = E_{DF} \cdot E_{SF} + \gamma$$

$$\gamma = \frac{(\dot{\rho}_2 - \dot{\rho}_1) \cdot (\dot{\Gamma}_2 \cdot \dot{\rho}_2 - \dot{\Gamma}_3 \cdot \dot{\rho}_3) + (\dot{\rho}_2 - \dot{\rho}_3) \cdot (\dot{\Gamma}_1 \cdot \dot{\rho}_1 - \dot{\Gamma}_2 \cdot \dot{\rho}_2)}{(\dot{\Gamma}_3 - \dot{\Gamma}_2) \cdot (\dot{\Gamma}_2 \cdot \dot{\rho}_2 - \dot{\Gamma}_1 \cdot \dot{\rho}_1) + (\dot{\Gamma}_1 - \dot{\Gamma}_2) \cdot (\dot{\Gamma}_3 \cdot \dot{\rho}_3 - \dot{\Gamma}_2 \cdot \dot{\rho}_2)}$$

The theoretical value of the reflection coefficient by the equivalent circuit when inserting each sample is as shown on the right side.

$$\dot{\Gamma}_i = \frac{\dot{Z}_{\Gamma_i} - Z_0}{\dot{Z}_{\Gamma_i} + Z_0} = \frac{1 - j\omega C_0 \cdot \dot{\epsilon}_{ri} \cdot Z_0 - j\omega C_f \cdot Z_0}{1 + j\omega C_0 \cdot \dot{\epsilon}_{ri} \cdot Z_0 + j\omega C_f \cdot Z_0}$$

The uncertainty of the measured value of S_{11} after calibration can be calculated by the formula shown on the right side.

$$u_c = \sqrt{\sum_{i=1}^3 \epsilon_{t_i}^2 \cdot u^2(\Gamma_i)} = \sqrt{\epsilon_{t_1}^2 \cdot u^2(\Gamma_1) + \epsilon_{t_2}^2 \cdot u^2(\Gamma_2) + \epsilon_{t_3}^2 \cdot u^2(\Gamma_3)}$$

$u(\Gamma_i)$: Uncertainty under each calibration condition

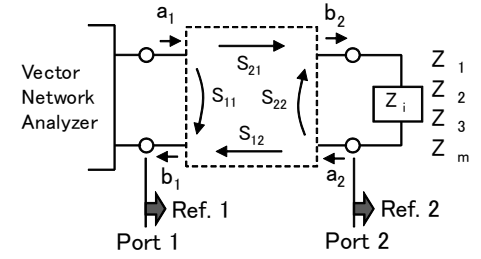
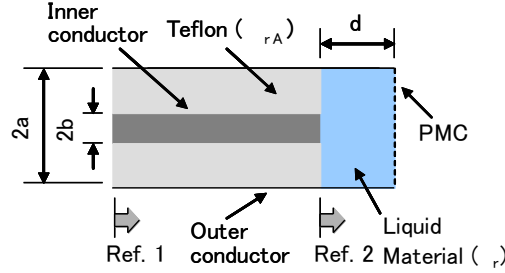
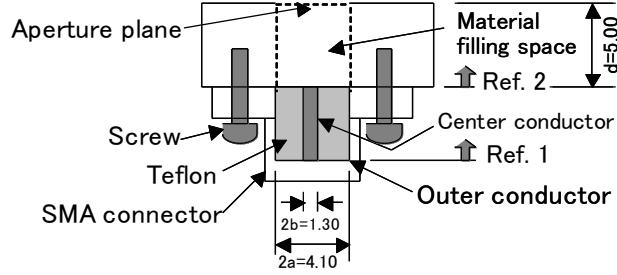
$$\epsilon_{t_i} = \frac{\partial \Gamma_{corr}}{\partial E_{DF}} \cdot \frac{\partial E_{DF}}{\partial \rho_i} \cdot \frac{\partial \rho_i}{\partial \Gamma_i} \cdot \epsilon_i + \frac{\partial \Gamma_{corr}}{\partial E_{SF}} \cdot \frac{\partial E_{SF}}{\partial \rho_i} \cdot \frac{\partial \rho_i}{\partial \Gamma_i} \cdot \epsilon_i + \frac{\partial \Gamma_{corr}}{\partial E_{RF}} \cdot \frac{\partial E_{RF}}{\partial \rho_i} \cdot \frac{\partial \rho_i}{\partial \Gamma_i} \cdot \epsilon_i$$

ϵ_{t_i} : Measurement error determined from uncertainty propagation theory when the reflection coefficient when inserting each reference material differs from the true value

$$\dot{\epsilon}_i = \dot{\Gamma}_i - \dot{\Gamma}_{i_ideal}$$

In this study, the above partial differentiation is carried out by the numerical analysis (The formula for calculating measurement uncertainty by the analytical partial differentiation has not been derived).

A Procedure for evaluation of the measurement uncertainty of S_{11} value after calibration for coaxial line with three reference materials and no short termination



$$\dot{\Gamma}_{corr} = \frac{a_2}{b_2} = \frac{\dot{\rho}_{meas} - \dot{E}_{DF}}{\dot{E}_{RF} + \dot{E}_{SF} \cdot (\dot{\rho}_{meas} - \dot{E}_{DF})}, \quad E_{SF} = \frac{\dot{\rho}_2 - \dot{\rho}_3 + \gamma \cdot (\dot{\Gamma}_3 - \dot{\Gamma}_2)}{\dot{\Gamma}_2 \cdot \dot{\rho}_2 - \dot{\Gamma}_3 \cdot \dot{\rho}_3}, \quad E_{DF} = \dot{\rho}_1 - \dot{\Gamma}_1 \cdot (E_{SF} \cdot \dot{\rho}_1 + \gamma)$$

$$E_{RF} = E_{DF} \cdot E_{SF} + \gamma$$

The uncertainty of the measured value of S_{11} after calibration

$$u_c = \sqrt{\sum_{i=1}^3 \varepsilon_{t_i}^2 \cdot u^2(\Gamma_i)} = \sqrt{\varepsilon_{t_1}^2 \cdot u^2(\Gamma_1) + \varepsilon_{t_2}^2 \cdot u^2(\Gamma_2) + \varepsilon_{t_3}^2 \cdot u^2(\Gamma_3)}$$

$u(\Gamma_i)$: Uncertainty under each calibration condition

$$\varepsilon_{t_i} = \frac{\partial \Gamma_{corr}}{\partial E_{DF}} \cdot \frac{\partial E_{DF}}{\partial \rho_i} \cdot \frac{\partial \rho_i}{\partial \Gamma_i} \cdot \varepsilon_i + \frac{\partial \Gamma_{corr}}{\partial E_{SF}} \cdot \frac{\partial E_{SF}}{\partial \rho_i} \cdot \frac{\partial \rho_i}{\partial \Gamma_i} \cdot \varepsilon_i + \frac{\partial \Gamma_{corr}}{\partial E_{RF}} \cdot \frac{\partial E_{RF}}{\partial \rho_i} \cdot \frac{\partial \rho_i}{\partial \Gamma_i} \cdot \varepsilon_i$$

ε_{t_i} : Measurement error determined from uncertainty propagation theory when the reflection coefficient when inserting each reference material differs from the true value

$$\dot{\varepsilon}_i = \dot{\Gamma}_i - \dot{\Gamma}_{i_ideal}$$

In this study, the partial differentiation is carried out by the numerical analysis (The formula for calculating measurement uncertainty by the analytical partial differentiation has not been derived).

1. The measurement error ε_i under each calibration condition is calculated by Eq. (4).
2. The small change of Γ_{corr} is calculated from the small change of E_{DF} , E_{SF} and E_{RF} by Eq. (1).
3. Small changes of E_{DF} , E_{SF} and E_{RF} are calculated from the small changes of ρ_i by Eq. (1).
4. The small change of ρ_i is calculated by Eq. (1) from the small change of Γ_i .
5. the measurement error ε_{t_i} considering the theory of propagation of measurement uncertainty is calculated by substituting the above values into Eq. (3).
6. The uncertainty $u(\Gamma_i)$ under each calibration condition is defined as the difference between the theoretical value and the measured value from the calculation result of ε_i (The measured value in this study is the reflection coefficient when inserting each sample after SOL calibration).
7. Item 5 measurement error ε_{t_i} and item 6 $u(\Gamma_i)$ are substituted into u_c in Eq. (2).

Comparison of jig calibration methods before insertion of sample and measurement of S_{11}

Method	Advantage	Weak point	Remarks
The jig is attached to the tip of the coaxial cable after calibration with a general SOL calibration kit [1]	A rigorous method, if the actual physical dimensions and the analytical model is matched	The effect of individual differences in jigs cannot be eliminated	An error occurs when moving the observation plane to the front of the sample
Calibration with short, open and one reference material [2]	Easy measurement by estimation formula	Ingenuity is required for realization of actual short	Technique used in commercially available coaxial probe methods such as Keysight Technology
Calibration with three reference materials [3]	Movement of the observation plane from the SOL calibration plane (Ref. 1) to the sample front surface (Ref. 2) is not required	Two kinds of liquids (true value of complex permittivity) are required	
Calibration with short, open and loaded [4]	Reference liquid is not required	Ingenuity is required to realize the actual load	

[1] K. Shibata, "Measurement of Complex Permittivity for Liquid Materials Using the Open-ended Cut-off Waveguide Reflection Method," IEICE Trans. Electron., Vol. E93-C, No. 11, pp. 1,621 – 1,629, 2010-11.

[2] K. Shibata, "S11 Calibration Method for a Coaxial-loaded Cut-off Circular Waveguide using SOM Termination," Proc. of 2020 IEEE Sensors Applications Symposium, IEEE SAS 2020, Kuala Lumpur, Malaysia, 2020-3.

[3] K. Shibata, "S11 Calibration Method for a Coaxial Line with Three Reference Materials and no Short Termination Condition for Dielectric Measurement in Liquids," Proc. of URSI AP-RASC 2019, New Delhi, India, 2019-3.

[4] K. Shibata, "S11 Calibration for a Coaxial-loaded Cut-off Circular Waveguide with SOL (short , open and load) Termination and Related Application to the Dielectric Measurement in Liquids," IEICE Tech. Rep., vol. 120, no. 54, MW2020-13, pp. 11-16, June 2020.

Verification of S_{11} calibration theory with three reference materials at 1.0, 1.5 and 3.0 GHz

Complex permittivity at 25°C and theoretical values of input impedance at the front surface of the material (Ref. 2) with the reference material inserted

Value	Frequency [GHz]		
	0.50	1.5	3.0
Complex permittivity of pure water	78.504 -j 1.912	78.108 -j 5.705	76.803 -j 11.206
Complex permittivity of methanol	35.957 -j 4.6560	30.927 -j 11.818	22.086 -j 15.092
Complex permittivity of air	1.0 -j 0.0	1.0 -j 0.0	1.0 -j 0.0
Mode matching method with pure water inserted Z_{1_ideal}	3.468596 -j 142.7852	3.469369 -j 46.7845	3.485887 -j 21.94313
Mode matching method with methanol inserted Z_{2_ideal}	39.2172 -j 305.566	39.7716 -j 104.3457	38.8407 -j 55.8549
Mode matching method with air inserted Z_{3_ideal}	0.00000 -j 9734.553	0.000000 -j 3243.967	0.000000 -j 1620.489
Equivalent circuit with pure water inserted Z_1	3.468596 -j 142.7852	3.469370 -j 46.7847	3.485889 -j 21.9431
Equivalent circuit with methanol inserted Z_2	39.2172 -j 305.5660	39.7716 -j 104.346	38.8407 -j 55.8549
Equivalent circuit with air inserted Z_3	-2.1854·10⁻² -j 9734.553	+4.398·10⁻⁴ -j 3243.97	-1.0850·10⁻³ -1620.489

The measured result of the complex permittivity of methanol by the cut-off circular waveguide reflection method in our institute is significantly different from the measured value by the coaxial probe method published by many other institutions

Accordingly, in this case, the complex permittivity measured by the cut-off circular waveguide reflection method was adopted

Measured input impedance on the SOL calibration plane (Ref. 1) with reference material insertion at 25°C

Value	Frequency [GHz]		
	0.50	1.5	3.0
Pure water Z_{corr1}	2.088336 -j 112.79212	2.097824 -j 21.19944	2.958538 -j 14.40730
Methanol Z_{corr2}	13.433887 -j 185.50422	14.062874 -j 50.94526	15.786494 -j 12.16781
Air Z_{corr3}	0.743282 -j 406.253174	0.262391 -j 130.00162	0.165109 -j 55.22374

Verification of input impedance calibration with reference materials inserted (25°C)

Value	Frequency [GHz]		
	0.50	1.5	3.0
Measured value for Ref. 1 Z_{meas1} after calibration with pure water inserted	2.247240 -j 111.2634	2.250545 -j 24.48425	3.135287 +j 12.065865
Calibration value for Ref. 2 Z_{corr1} for ρ_{meas1} and Eq. (1) with pure water inserted	3.468596 -j 142.7852	3.469373 -j 46.7848	3.485887 -j 21.9431
Measured value for Ref. 1 Z_{meas2} after calibration with methanol inserted	13.3781433 -j 174.7857	14.0628738 -j 50.94525	15.7864943 -j 12.167809
Calibration value for Ref. 2 Z_{corr2} for ρ_{meas2} and Eq. (1) with methanol inserted	39.2173 -j 305.5665	39.77165 -j 104.3457	38.84075 -j 55.8549
Measured value for Ref. 1 Z_{meas3} after calibration with air inserted	1.256953 -j 416.0070	0.349457 -j 133.2416	0.190314 -j 56.7360
Calibration value for Ref. 2 Z_{corr3} for ρ_{meas3} and Eq. (1) with air inserted	-0.0676193 -j 9734.625	0.0092236 -j 3243.971	-0.00039843 -j 1620.4885

Budget sheet for evaluation of measurement uncertainty

Reflection coefficient, measurement error and uncertainty at the front surface of the sample (Ref. 2) with the reference material inserted

Reference material 1 (pure water, 25°C)

Reference material 2 (methanol, 25°C)

Value	Frequency [GHz]		
	0.50	1.5	3.0
Measured input impedance with another calibration method Z	+3.8796360	+3.771432	+3.6705978
	-j 160.5367	-j 52.4138	-j 24.64155
Theoretical input impedance with the mode matching method Z_{ideal3}	+3.468596	+3.469369	+3.48589
	-j 142.7852	-j 46.78456	-j 21.9431
Measured reflection coefficient with another calibration method Γ	+0.81210	-0.04637	-0.53884
	-j 0.55985	-j 0.92956	-j 0.70652
Theoretical reflection coefficient with the mode matching method Γ_{ideal3}	+0.76999	-0.05927	-0.60030
	-j 0.611422	-j 0.92684	-j 0.65654
Measurement error ϵ_3	+4.2109·10 ⁻²	+1.0563·10 ⁻¹	+7.0853·10 ⁻²
	+j 5.437·10 ⁻²	-j 2.721·10 ⁻³	-j 5.964·10 ⁻²
Uncertainty $u(\Gamma_3)$	+4.2109·10 ⁻²	+1.0563·10 ⁻¹	+7.0853·10 ⁻²
	+j 5.4374·10 ⁻²	-j 2.721·10 ⁻³	-j 5.964·10 ⁻²

Value	Frequency [GHz]		
	0.50	1.5	3.0
Measured input impedance with another calibration method Z	+41.7726479	+42.5391083	+40.680000
	-j 333.30685	-j 112.77932	-j 59.47895
Theoretical input impedance with the mode matching method Z_{ideal2}	+39.21722	+39.771641	+38.8407478
	-j 305.563	-j 104.3457	-j 55.854939
Measured reflection coefficient at the front surface of the sample (Ref. 2) with another calibration method Γ	+0.92321	+0.56519	+0.22895
	-j 0.27888	-j 0.52991	-j 0.50575
Theoretical reflection coefficient with the mode matching method Γ_{ideal2}	+0.92321	+0.569189	+0.22895
	-j 0.27888	-j 0.52927	-j 0.50575
Measurement error ϵ_2	+1.12604·10 ⁻²	+3.89948·10 ⁻²	+3.5682·10 ⁻²
	+j 2.26757·10 ⁻²	+j 2.08132·10 ⁻²	+j 1.451·10 ⁻³
Uncertainty $u(\Gamma_2)$	+1.12604·10 ⁻²	+3.89948·10 ⁻²	+3.5682·10 ⁻²
	+j 2.26757·10 ⁻²	+j 2.08132·10 ⁻²	+j 1.451·10 ⁻³

Reference material 3 (air, 25°C)

Measured input impedance Z_{corr1} (25°C) for Ref. 1 (SOL calibration plane) with unknown materials inserted after calibration with three reference materials

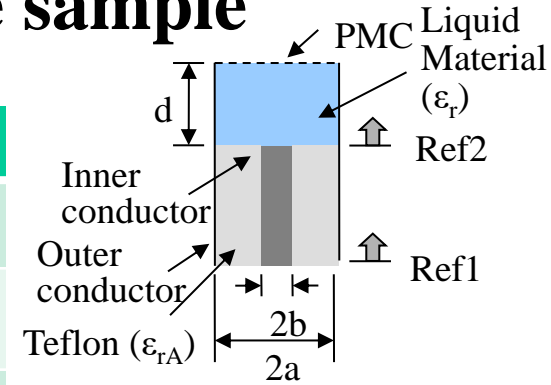
Value	Frequency [GHz]		
	0.50	1.5	3.0
Measured input impedance with another calibration method Z	+454.21643	+158.32234	+78.998062
	-j 10108.189	-j 3417.362	-j 1626.826
Theoretical input impedance with the mode matching method Z_{ideal3}	0.0000	0.00000	0.000
	-j 9734.554	-j 3243.967	-j 1620.489
Measured reflection coefficient with another calibration method Γ	+0.99951	+0.99822	+0.99516
	-j 0.00987	-j 0.02915	-j 0.06109
Theoretical reflection coefficient with the mode matching method Γ_{ideal3}	+0.99951	+0.99952	+0.99810
	-j 0.00987	-j 0.003082	-j 0.06165
Measurement error ϵ_3	-4.39493·10 ⁻⁴	-1.3022·10 ⁻³	-2.9414·10 ⁻³
	+j 4.039·10 ⁻³	+j 1.665·10 ⁻³	+j 5.658·10 ⁻³
Uncertainty $u(\Gamma_3)$	-4.39493·10 ⁻⁴	-1.3022·10 ⁻³	-2.9415·10 ⁻³
	+j 4.040·10 ⁻³	+j 1.665·10 ⁻³	+j 5.658·10 ⁻³

Value	Frequency [GHz]		
	0.50	1.5	3.0
Unknown material 1 Pure water	+2.088335	+2.243403	+3.115806
	-j 112.7921	-j 24.9937	+j 11.80240
Unknown material 2 Methanol	+13.433887	+14.21072	+15.599522
	-j 185.5042	-j 54.65093	-j 14.371228
Unknown material 3 Ethanol	+38.069847	+25.75860	+14.06677
	-j 228.0731	-j 85.07299	-j 38.3509

Evaluation of measurement uncertainty of S_{11} after calibration of a cut-off circular waveguide with three reference materials in front of the sample

Pure water inserted as an unknown material (25°C)

Value	Frequency [GHz]		
	0.50	1.5	3.0
With pure water inserted ϵ_{t_1}	$-1.4478 \cdot 10^{-1}$ $-1.8699 \cdot 10^{-1}$	$-3.3683 \cdot 10^{-1}$ $-1.7616 \cdot 10^{-3}$	$-2.2883 \cdot 10^{-1}$ $+2.1057 \cdot 10^{-1}$
With methanol inserted ϵ_{t_2}	$-3.4185 \cdot 10^{-2}$ $-6.5227 \cdot 10^{-2}$	$-9.7598 \cdot 10^{-2}$ $-3.8679 \cdot 10^{-2}$	$-7.5438 \cdot 10^{-2}$ $+3.1608 \cdot 10^{-2}$
With air inserted ϵ_{t_3}	$+1.1607 \cdot 10^{-3}$ $-1.1004 \cdot 10^{-3}$	$+1.4633 \cdot 10^{-3}$ $-1.2695 \cdot 10^{-3}$	$-5.3887 \cdot 10^{-5}$ $+1.2075 \cdot 10^{-3}$
Theoretical reflection coefficient with the mode matching method Γ_{ideal}	+0.769990 -j 0.61422	-0.05927 -j 0.92684	-0.60030 -j 0.65654
Correction value for reflection coefficient after calibration Γ_{corr}	+0.769993 -j 0.614222	-0.0592675 -j 0.926837	-0.6096895 -j 0.646884
Measurement uncertainty u_c	$6.1087 \cdot 10^{-3}$ $1.0275 \cdot 10^{-2}$	$3.5783 \cdot 10^{-2}$ $8.0645 \cdot 10^{-4}$	$1.6435 \cdot 10^{-2}$ $1.2558 \cdot 10^{-2}$



$$u_c = \sqrt{\sum_{i=1}^3 \epsilon_{t_i}^2 \cdot u^2(\Gamma_i)}$$

$$\epsilon_{t_i} = \frac{\partial \Gamma_{corr}}{\partial E_{DF}} \cdot \frac{\partial E_{DF}}{\partial \rho_i} \cdot \frac{\partial \rho_i}{\partial \Gamma_i} \cdot \epsilon_i$$

$$+ \frac{\partial \Gamma_{corr}}{\partial E_{SF}} \cdot \frac{\partial E_{SF}}{\partial \rho_i} \cdot \frac{\partial \rho_i}{\partial \Gamma_i} \cdot \epsilon_i$$

$$+ \frac{\partial \Gamma_{corr}}{\partial E_{RF}} \cdot \frac{\partial E_{RF}}{\partial \rho_i} \cdot \frac{\partial \rho_i}{\partial \Gamma_i} \cdot \epsilon_i$$

$$\dot{\epsilon}_i = \dot{\Gamma}_i - \dot{\Gamma}_{i_ideal}$$

Confirmed the measurement uncertainty of S_{11} of the same order as at the time of calibration with a normal SMA type SOL calibration kit by adopting the calibration with three standard materials.

Individual differences in jigs can be eliminated by adopting the calibration of S_{11} on the front of the sample with three reference materials.

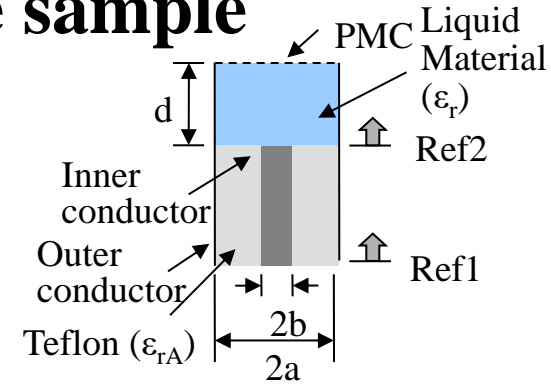
At that time, the reference plane does not need to be moved from the SOL calibration plane. 27

Accordingly, it is expected to improve the uncertainty under the dielectric measurement in liquids.

Evaluation of measurement uncertainty of S_{11} after calibration of a cut-off circular waveguide with three reference materials in front of the sample

Methanol inserted as an unknown material (25°C)

Value	Frequency [GHz]		
	0.50	1.5	3.0
With pure water inserted ε_{t1}	$-1.3622 \cdot 10^{-2}$ $-1.8088 \cdot 10^{-1}$	$-2.88356 \cdot 10^{-1}$ $-3.7896 \cdot 10^{-2}$	$-2.5019 \cdot 10^{-1}$ $+2.1689 \cdot 10^{-1}$
With methanol inserted ε_{t2}	$-3.3702 \cdot 10^{-2}$ $-6.7517 \cdot 10^{-2}$	-0.115849 $-6.17681 \cdot 10^{-2}$	$-6.6657 \cdot 10^{-2}$ $-4.0535 \cdot 10^{-3}$
With air inserted ε_{t3}	$+1.2805 \cdot 10^{-3}$ $-1.1874 \cdot 10^{-3}$	$+3.76967 \cdot 10^{-3}$ $-3.59736 \cdot 10^{-3}$	$-4.2908 \cdot 10^{-4}$ $+4.3845 \cdot 10^{-3}$
Theoretical reflection coefficient with the mode matching method Γ_{ideal}	+0.92321 -j 0.2789	+0.56519 -j 0.52991	+0.22895 -j 0.50575
Correction value for reflection coefficient after calibration Γ_{corr}	+0.92321 -j 0.7888	+0.56519 -j 0.5299	+0.23071 -j 0.50574
Measurement uncertainty u_c	$5.7489 \cdot 10^{-3}$ $9.9538 \cdot 10^{-3}$	$3.0290 \cdot 10^{-2}$ $1.2897 \cdot 10^{-3}$	$1.7886 \cdot 10^{-2}$ $1.2934 \cdot 10^{-2}$



$$u_c = \sqrt{\sum_{i=1}^3 \varepsilon_{t-i}^2 \cdot u^2(\Gamma_i)}$$

$$\varepsilon_{t-i} = \frac{\partial \Gamma_{corr}}{\partial E_{DF}} \cdot \frac{\partial E_{DF}}{\partial \rho_i} \cdot \frac{\partial \rho_i}{\partial \Gamma_i} \cdot \varepsilon_i$$

$$+ \frac{\partial \Gamma_{corr}}{\partial E_{SF}} \cdot \frac{\partial E_{SF}}{\partial \rho_i} \cdot \frac{\partial \rho_i}{\partial \Gamma_i} \cdot \varepsilon_i$$

$$+ \frac{\partial \Gamma_{corr}}{\partial E_{RF}} \cdot \frac{\partial E_{RF}}{\partial \rho_i} \cdot \frac{\partial \rho_i}{\partial \Gamma_i} \cdot \varepsilon_i$$

$$\dot{\varepsilon}_i = \dot{\Gamma}_i - \dot{\Gamma}_{i-ideal}$$

Confirmed the measurement uncertainty of S_{11} of the same order as at the time of calibration with a normal SMA type SOL calibration kit by adopting the calibration with three standard materials. Individual differences in jigs can be eliminated by adopting the calibration of S_{11} on the front of the sample with three reference materials.

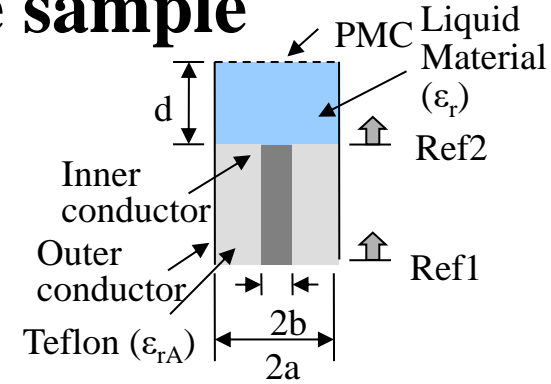
At that time, the reference plane does not need to be moved from the SOL calibration plane. 28

Accordingly, it is expected to improve the uncertainty under the dielectric measurement in liquids.

Evaluation of measurement uncertainty of S_{11} after calibration of a cut-off circular waveguide with three reference materials in front of the sample

Ethanol inserted as an unknown material (25°C)

Value	Frequency [GHz]		
	0.50	1.5	3.0
With pure water inserted ε_{t1}	$-1.3077 \cdot 10^{-1}$	$-1.8339 \cdot 10^{-1}$	$-1.8173 \cdot 10^{-1}$
	$-1.7264 \cdot 10^{-1}$	$+4.1399 \cdot 10^{-2}$	$+1.2199 \cdot 10^{-1}$
With methanol inserted ε_{t2}	$-3.3076 \cdot 10^{-2}$	-0.10673	$-3.6426 \cdot 10^{-3}$
	$-6.6831 \cdot 10^{-2}$	$-5.9517 \cdot 10^{-2}$	$+1.4168 \cdot 10^{-2}$
With air inserted ε_{t3}	$+1.3052 \cdot 10^{-3}$	$+4.0143 \cdot 10^{-3}$	$-3.4566 \cdot 10^{-3}$
	$-1.2052 \cdot 10^{-3}$	$-4.8051 \cdot 10^{-3}$	$+1.3067 \cdot 10^{-3}$
Theoretical reflection coefficient with the mode matching method Γ_{ideal}	+0.905604	+0.729956	+0.646845
	-j 0.18519	-j 0.23880	-j 0.275584
Correction value for reflection coefficient after calibration Γ_{corr}	+0.91691	+0.73792	+0.64955
	-j 0.175422	-j 0.234101	+j 0.26323
Measurement uncertainty u_c	$5.5191 \cdot 10^{-3}$	$1.9814 \cdot 10^{-2}$	$1.2877 \cdot 10^{-2}$
	$9.5084 \cdot 10^{-3}$	$1.2439 \cdot 10^{-3}$	$7.2747 \cdot 10^{-3}$



$$u_c = \sqrt{\sum_{i=1}^3 \varepsilon_{t-i}^2 \cdot u^2(\Gamma_i)}$$

$$\varepsilon_{t-i} = \frac{\partial \Gamma_{corr}}{\partial E_{DF}} \cdot \frac{\partial E_{DF}}{\partial \rho_i} \cdot \frac{\partial \rho_i}{\partial \Gamma_i} \cdot \varepsilon_i$$

$$+ \frac{\partial \Gamma_{corr}}{\partial E_{SF}} \cdot \frac{\partial E_{SF}}{\partial \rho_i} \cdot \frac{\partial \rho_i}{\partial \Gamma_i} \cdot \varepsilon_i$$

$$+ \frac{\partial \Gamma_{corr}}{\partial E_{RF}} \cdot \frac{\partial E_{RF}}{\partial \rho_i} \cdot \frac{\partial \rho_i}{\partial \Gamma_i} \cdot \varepsilon_i$$

$$\dot{\varepsilon}_i = \dot{\Gamma}_i - \dot{\Gamma}_{i-ideal}$$

Confirmed the measurement uncertainty of S_{11} of the same order as at the time of calibration with a normal SMA type SOL calibration kit by adopting the calibration with three standard materials.

Individual differences in jigs can be eliminated by adopting the calibration of S_{11} on the front of the sample with three reference materials.

At that time, the reference plane does not need to be moved from the SOL calibration plane. 29

Accordingly, it is expected to improve the uncertainty under the dielectric measurement in liquids.

Summary

The following work was carried out for the purpose of improving the uncertainty in the dielectric measurement from S_{11} value when liquids were inserted into the open-ended cut-off circular waveguide.

S_{11} on the front surface of the sample was calibrated at each frequency of 0.50, 1.5 and 3.0 GHz using three reference materials of pure water, methanol and air (open) and without short termination.

For this purpose, S_{11} on the front surface of the sample after calibration was first obtained when pure water, methanol, and ethanol were inserted into the jig as unknown materials.

Re-confirmed that S_{11} on the front surface of the sample could be calibrated with the three reference materials

Uncertainty of the measured S_{11} values after calibration was calculated when the measured S_{11} values when the three reference substances were inserted deviated from the theoretical values.

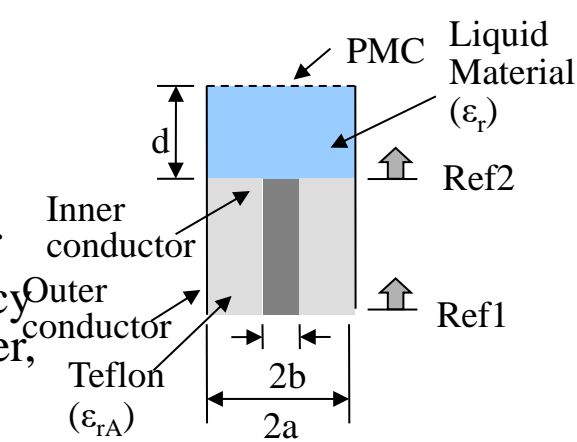
Confirmed the measurement uncertainty of S_{11} of the same order as at the time of calibration with a normal SMA type SOL calibration kit by adopting the calibration with three standard materials in any case of inserting pure water, methanol or ethanol as unknown materials.

Individual differences in jigs can be eliminated by adopting the S_{11} calibration on the front of the sample with three reference materials. The reference plane does not need to be moved from the SOL calibration plane. It is expected to improve the uncertainty under the dielectric measurement.

In the future, it is necessary to **extend to the uncertainty of dielectric measurement in liquids by the cut-off circular waveguide** including the above-mentioned uncertainty when calibrating S_{11} .

Meanwhile, **the measured value of the permittivity of methanol by the cutoff circular waveguide reflection method is different from the Debye dispersion equation corrected by the published coaxial probe method.**

Determination of the true value from the above measurements is required.



Issues for standardization of the method

Establishment of calibration method for S_{11} in front of sample with short, open and one kind of reference material

Comparison of measurement uncertainty between this method and other methods such as the coaxial probe method in various measurement procedures

A round robin test (an inter laboratory test performed independently several times) is needed by supplying the estimation software and the measurement manual to another institutes for confirmation the effectiveness of proposed dielectric measurement method.

This requires multiple independent engineers to perform the test using this method on different equipment.

